Synthesis, computational study and glycosidase inhibitory activity of polyhydroxylated conidine alkaloids—a bicyclic iminosugar†

Shrihari P. Sanap,[a] Sougata Ghosh,[b] Amit M. Jabgunde,[a] Rahul V. Pinjari,[c] Shridhar P. Gejji,[c] Shailza Singh,[b] Balu A. Chopade[b] and Dilip D. Dhavale*[a]

Received 26th March 2010, Accepted 13th May 2010
First published as an Advance Article on the web 2nd June 2010
DOI: 10.1039/c004690f

New bicyclic conidine iminosugars **1d** and **1e** were synthesized from D-glucose. Thus, D-glucose was converted to sugar β-amino acids **3a** and **3b** in good yields. Individual treatment of **3a**/**3b** with the Mukaiyama reagent afforded sugar β-lactams **4a**/**4b** that on reduction with $LiAlH_4/AlCl_3$ gave azetidines **5a**/**5b** with a sugar appendage. Reductive aminocyclization of sugar azetidines **5a**/**5b** afforded the corresponding conidine iminosugars **1d**/**1e**. Based on the ^{1}H NMR and DFT calculation studies the conformation of **1d** was assigned as half chair **A2** and that of **1e** as a boat **B2**. The glycosidase inhibitory activities of **1d** and **1e** such as α-mannosidase, α-glucosidase and α-galactosidase were studied. The α-amylase activity was compared with acarbose. Compound **1d** was found to be a moderate inhibitor of glycosidases while **1e** was noticed to be a good inhibitor of α-mannosidase and a moderate inhibitor of other glycosidases. These results were substantiated by molecular docking studies using WHAT IF software and the AUTODOCK 3.0 program.

Introduction

Glycosidic bond cleavage plays a pivotal role in a wide range of metabolic processes that include digestion, glycoconjugate lysosomal catabolism and glycoprotein biosynthesis/degradation within the endoplasmic reticulum (ER).[1] However, increased levels of glycosidases like α-mannosidase, α-galactosidase and α-glucosidase leads to severe pathological complications. For example, α-mannosidase is involved in the *N*-glycosylation pathway[2] by trimming $Glc_3Man_9GlcNAc_2$ moieties in human ER, however, abnormalities in this pathway lead to disease progression, metastasis and poor clinical outcome in the case of breast, colon and skin cancers.[3] α-Galactosidase regulates catabolism of glycosphingolipids in the lysosome and any disorder in this process causes lysosomal storage disease (LSD)[4] and Fabry's disease.[5] α-Glucosidase is involved in non-insulin dependent diabetes mellitus (NIDDM) or type II diabetes[6] and inhibition of α-glucosidase/α-amylase significantly decreases post-prandial hyperglycemia (PPHG) in the treatment of type II diabetic patients. Thus, discovery of a suitable inhibitor of the glycosidase process is a challenge in the search for a potent therapeutic agent for the treatment of diseases such as cancer,[7] diabetes[8] and viral infections including AIDS.[9] The mechanism of glycosidase inhibitors includes competitive, non-/un-competitive and mixed inhibition of enzymes. In general, enzyme catalyzed glycosidic bond cleavage of pyranosides is mediated by two catalytic carboxylic acid residues and typically proceeds through a positively charged oxo-carbenium ion transition state.[10] Many natural and synthetic glycosidase inhibitors mimic the charge buildup and/or the conformational distortion of the transition state and thus act as glycosidase inhibitors. In this direction, the search for an α-glucosidase inhibitor led to the discovery of acarbose (trade names: Glucobay/Precose/Prandase)—a pseudotetrasaccharide as a potent sucrase inhibitor, voglibose (trade name: Voglib)—a polyhydroxylated aminocyclitol and *N*-hydroxyethyl-1-deoxynojirimycin (Trade name: Glyset/Miglitol)—a synthetic iminosugar used in the treatment of type II diabetes mellitus.[11]

Iminosugars are polyhydroxylated mono- or bi-cyclic compounds with the nitrogen atom in the ring for monocyclic and at the ring fusion for bicyclic compounds with promising glycosidase inhibitory activity.[12] A number of bi-cyclic iminosugars such as six–five ring fused indolizidine (castanospermine, swainsonine, lentiginosine), six–six ring fused quinolizidine, five–five ring fused pyrrolizidine iminosugars (australine, casuarine, hyacinthacine) and seven–five ring fused perhydroazaazulenes have been either isolated or synthesized and evaluated for their glycosidase inhibitory activity. However, six–four ring fused iminosugars are rare and only one example of a β-lactam-iminosugar hybrid **1a** (Fig. 1), which is a competitive potent galactosidase inhibitor, has been reported by Pandey *et al.*[13] In general, the six–four ring fused compounds with nitrogen atom at the ring fusion of type **1b** are called conidine[14] alkaloids and its 25 oligomer is known to be heparin antagonist.[15] Although, a few examples of alkyl substituted conidines are known;[16] polyhydroxylated conidines of general type **1c** that resembles bi-cyclic iminosugars, to the best of our knowledge, are unknown. As a part of our continuing interest in mono- and bi-cyclic iminosugars,[17] we are reporting herewith the synthesis, computational studies and glycosidase inhibitory

[a]*Garware Research Centre, Department of Chemistry, University of Pune, Pune-411007, India. E-mail: ddd@chem.unipune.ernet.in; Fax: +91-20-25691728*
[b]*Institute of Bioinformatics and Biotechnology, University of Pune, Pune-411007, India*
[c]*Division of Physical Chemistry, Department of Chemistry, University of Pune, Pune-411007, India*

† Electronic supplementary information (ESI) available: General experimental methods, copies of the ^{1}H and ^{13}C NMR spectra of compounds **3a**, **3b**, **4a**, **4b**, **5a**, **5b**, **1d** and **1e**, data for DFT calculations of compound **1d** and **1e**, calculated ^{1}H NMR and coupling constants for compound **1d** and **1e**, molecular docking of compound **1e** with human mannosidase (PDB: 1FO3). See DOI: 10.1039/c004690f

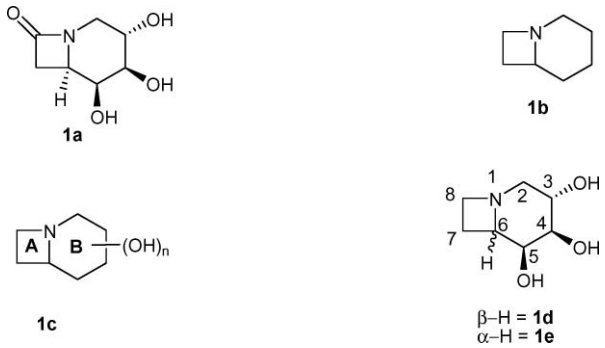

Fig. 1 Conidine iminosugars.

activity of new analogues of constrained polyhydroxylated conidine iminosugars **1d** and **1e**. It was anticipated that in **1d** and **1e**, the ring nitrogen atom at physiological pH will mimic the positive charge of the oxo-carbenium ion intermediate and the conformationally constrained azetidine ring **A** will induce the polyhydroxylated piperidine ring **B** to adopt a nearly half-chair conformation—a transition state required to mimic the enzymes in the glycosidase inhibition process. Such a restricted conformation with a polyhydroxylated framework, recognized by an enzyme, may increase the potency by lowering the entropic barrier to complex formation making these molecules promising glycosidase inhibitors.

Result and discussion

Our synthetic approach starts from the L-*ido* and D-*gluco* configured β-aminoesters **2a** and **2b** (Scheme 1), which were prepared in grams quantity from D-glucose as reported earlier by us.[18] In the next step, the L-*ido* configured β-aminoester **2a** was hydrolyzed with lithium hydroxide in methanol–water at 0 °C to room temperature to give β-amino acid **3a**[19] in 98% yield as a white solid. Treatment of **3a** with 2-chloro-1-methylpyridinium iodide (Mukaiyama reagent)[20] and triethylamine in dichloromethane at 25 °C afforded sugar β-lactam **4a** as a white solid in 89% yield. Reduction of β-lactam **4a** was attempted with various reagents such as DIBAL-H, $LiAlH_4$, 9-BBN and BH_3–THF. However, a better result in high yield was achieved with chlorohydroalane[21] reagent, prepared *in situ* from $LiAlH_4 : AlCl_3$ (3 : 1). Thus, reaction of **4a** with chlorohydroalane in anhydrous THF at –10 °C to 0 °C, yielded four membered azetidine compound **5a** with sugar appendage in 83% yield. In the final step, opening of the 1,2-acetonide functionality in **5a** with TFA : water (3 : 2) at 0 °C to room temperature afforded the hemiacetal (as evident from the ^{1}H NMR of the crude product) which on hydrogenation with H_2, 10% Pd/C at room temperature undergoes reductive aminocyclization[22] to give polyhydroxylated conidine iminosugar **1d** in 78% yield. The ^{1}H and ^{13}C NMR spectra were found to be consistent with the structure. While targeting the synthesis of polyhydroxylated 6a-*epi*-conidine **1e**, the same sequence of reaction was repeated with D-*gluco* configured β-aminoester **2b**. Thus, reaction of **2b** with LiOH in methanol–water at 0 °C to room temperature afforded β-amino acid **3b** in 96% yield that on treatment with Mukaiyama reagent at 25 °C gave β-lactam **4b** as a white solid in 91% yield. Reduction of β-lactam **4b** using chlorohydroalane at –10 °C to 0 °C afforded sugar azetidine **5b**

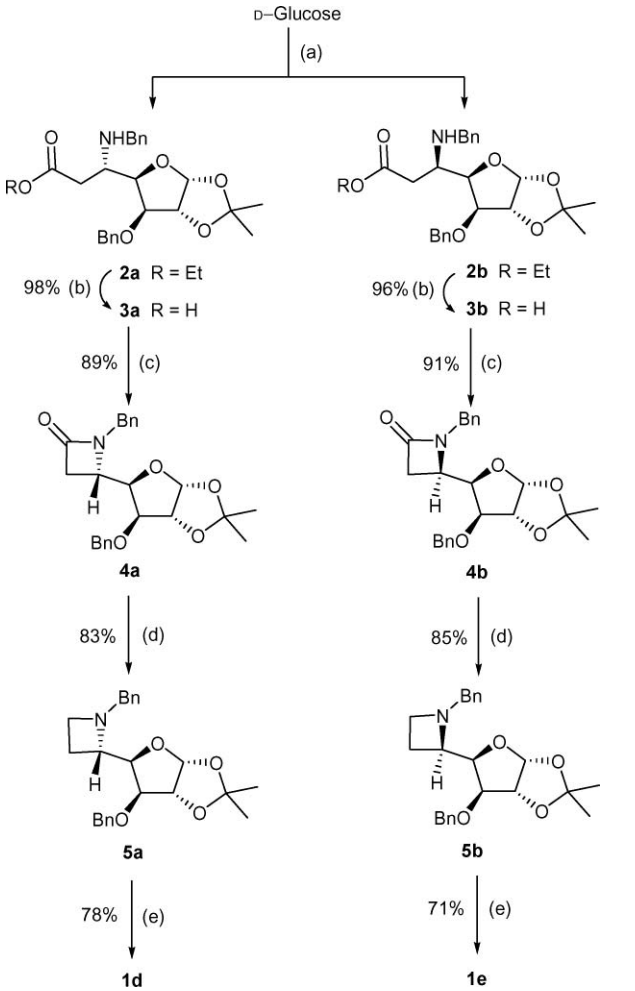

Scheme 1 *Reagents and conditions*: (a) Ref. 18; (b) $LiOH{\cdot}H_2O$, MeOH–H_2O, 0 °C to rt, 2 h; (c) 2-chloro-1-methylpyridinium iodide, Et_3N, dry CH_2Cl_2, 25 °C, 2 h; (d) $LiAlH_4/AlCl_3$, anhyd. THF, –10 °C to 0 °C, 10 min; (e) (i) TFA/H_2O (3 : 2), 0 °C to rt, 4 h; (ii) H_2, 10% Pd/C, MeOH, 80 psi, rt, 5 days.

as a white solid in 85% yield. In the final step, hydrolysis of the 1,2-acetonide functionality in **5b** and reductive aminocyclization using H_2, 10% Pd/C afforded conidine iminosugar **1e** in 71% yield.

Conformational study

In bicyclic iminosugars, the binding ability and their function as glycosidase inhibitors depend on their conformation. For example, an indolizidine iminosugar (six–five ring fused system) namely 1-deoxy-castanospermine exists in the $^8C_5$ conformation **I** (Fig. 2) and exhibits potent enzyme inhibition toward the α- and β-glucosidase and α-mannosidase; whereas 1-deoxy-8a-*epi*-castanospermine exists in the $^5C_8$ conformation **II** and shows selective inhibition of α- and β-galactosidase and β-glucosidase.[23,24] In the case of conidine iminosugars **1d** and **1e** (six–four ring fused systems), the ^{1}H NMR spectra were found to be dramatically different and knowing that the four membered fused azetidine ring system will change the conformation of the six membered piperidine ring, it is expected that both target molecules could exist in different conformations.

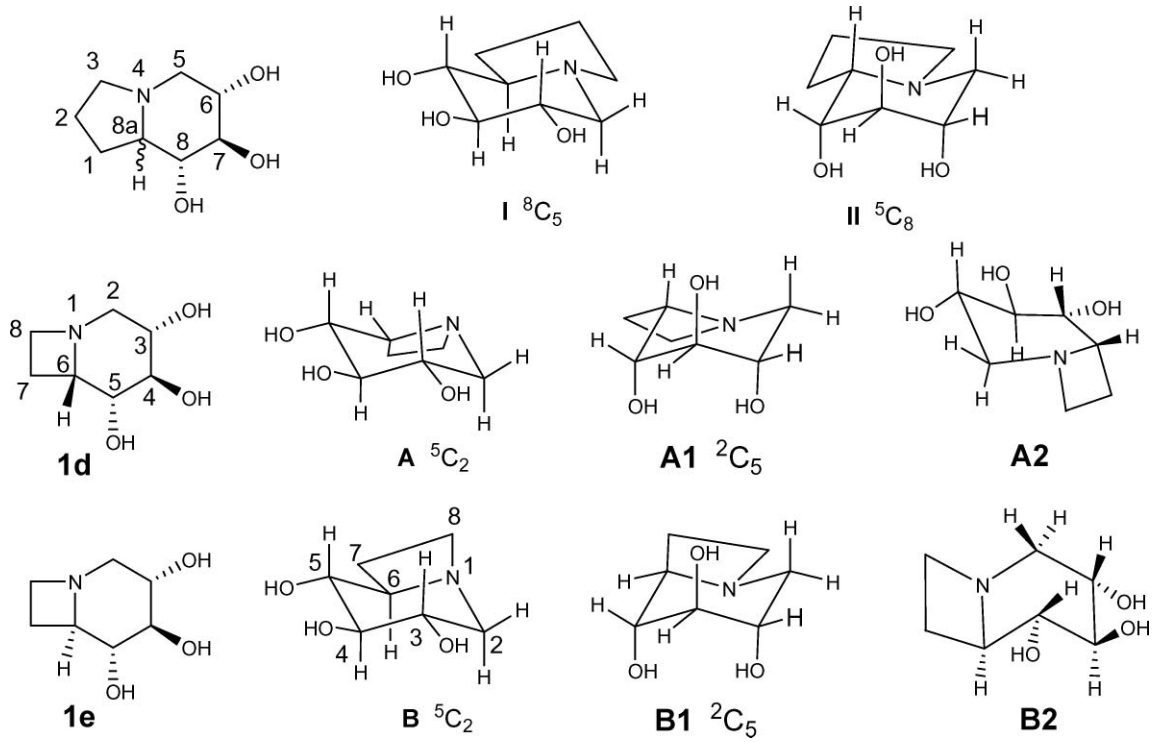

Fig. 2 Conformations of compounds **1d** and **1e**.

Table 1 ^{1}H NMR Spectra of **1d** and **1e**

	1d	**1e**
H-2a	3.34 (dd) $J_{2a,2e} = 12.6$ Hz $J_{2a,3a} = 11.0$ Hz	3.25 (dd) $J_{2a,2e} = 13.5$ Hz $J_{2a,3a} = 6.0$ Hz
H-2e	3.63 (dd) $J_{2a,2e} = 12.6$ Hz $J_{2e,3a} = 5.0$ Hz	3.43 (dd) $J_{2a,2e} = 13.5$ Hz $J_{2e,3a} = 3.3$ Hz
H-3	4.88–5.05 (m)	4.06–4.14 (m)
H-4	3.90 (t) $J_{4,3} = J_{4,5} = 6.9$ Hz	3.56 (dd) $J_{4,5} = 8.2$ Hz $J_{4,3} = 4.8$ Hz
H-5	3.95 (dd) $J_{5,4} = 6.9$ Hz $J_{5,6} = 6.0$ Hz	4.14–4.27 (m)
H-6	3.67–3.76 (m)	4.27–4.36 (m)
H-7a	2.44–2.58 (m)	2.34–2.50 (m)
H-7e	2.78–2.96 (m)	2.74–2.90 (m)
H-8a	3.82 (dt) $J_{8a,8e} = J_{8a,7a} = 10.0$ Hz $J_{8a,7e} = 4.7$ Hz	4.14–4.27 (m)
H-8e	4.45 (dt) $J_{8a,8e} = J_{8a,7e} = 10.0$ Hz $J_{8e,7a} = 8.8$ Hz	4.14–4.27 (m)

In order to assign the conformations, we studied the ^{1}H NMR spectra of **1d** and **1e** and the chemical shifts as well as the coupling constants obtained by the decoupling experiments and are given in Table 1. For compound **1d**, we assumed three conformations **A**, **A1** and **A2** (Fig. 2). In the ^{1}H NMR spectrum of **1d**, the H-2a proton appeared as a doublet of doublets with geminal and vicinal coupling constants of 12.6 Hz and 11.0 Hz, respectively. The large vicinal coupling constant $J_{2a,3a} = 11.0$ Hz requires the axial–axial relative orientation of H-2 and H-3 and therefore H-3 was assigned the axial orientation. This established the possibility of conformation **A** and ruled out conformation **A1**. In the precursor **5a**, the relative stereochemistry of H-2/H-3 and H-3/H-4 is *trans* and assuming that the same stereochemistry is retained in compound **1d**, the H-3/H-4 and H-4/H-5 should have axial–axial orientation. In accordance with this, H-4 appeared as a triplet ($J_{4a,3a} = J_{4a,5a} = 6.9$ Hz). The relatively small coupling constant for axially oriented H-3/H-4 ($J_{3a,4a} = 6.9$ Hz) required little distortion from the usual chair conformation of the piperidine ring. Thus, the dihedral angle of ~160° between the H-3 and H-4 protons (rather than the 180° in axial–axial) accounts for coupling constant of 6.9 Hz. In agreement with this, the axially oriented H-5 showed a doublet of doublets with $J_{4a,5a} = 6.9$ Hz and $J_{5a,6e} = 6.0$ Hz wherein, the relatively large coupling constant for axial–equatorial protons indicates a dihedral angle between H-5a and H-6e ~10°. This ruled out conformation **A1**. To account for these features, the half chair conformation **A2** was assigned to **1d** wherein, the fused four membered strained azetidine ring forced the piperidine ring to adopt a distorted half chair conformation.

In case of **1e**, three conformers **B**, **B1** and **B2** (Fig. 2) were considered. In the ^{1}H NMR of **1e**, one of the H-2 appeared as a doublet of doublets with geminal coupling constants of 13.5 Hz ($J_{2a,2e}$) and a vicinal coupling constant of 6.0 Hz ($J_{2a,3}$) while the other H-2 appeared as a doublet of doublets with coupling constants of 13.5 Hz and 3.3 Hz. The small vicinal coupling constant of $J_{2e,3e} = 3.3$ Hz ruled out the $^{5}C_2$ conformation **B** as it requires a large coupling constant between the axially oriented H-2/H-3 protons. To decide between conformations **B1** and **B2**, we considered the H-4 proton. In conformation **B1**, the H-4 is equatorial and is expected to show a doublet of doublets with small coupling constants. However, H-4 showed a doublet of doublets with $J_{4,5} = 8.2$ Hz and $J_{4,3} = 4.8$ Hz. The appearance of H-4 with a large coupling constant of $J_{4,5} = 8.2$ Hz ruled out the $^{2}C_5$

conformation **B1**. To account for this feature, we assumed the most probable boat conformation **B2** wherein the quasi-axially oriented H-4 has a large coupling constant of 8.2 Hz with the quasi-axial H-5 and a small coupling constant of 4.8 Hz with the quasi-equatorial H-3. In accordance with this, the H-5 showed a doublet of doublets with large coupling constants of 8.2 Hz with H-4 and 9.3 Hz with H-6 suggesting that the ring fusion proton (H-6) is quasi-axial. Thus, the boat conformation **B2** was assigned to compound **1e** wherein the two fused rings are the farthest away from each other and –OH groups are positioned either quasi-equatorial or quasi-axial. Thus, based on the ^{1}H NMR studies, conidine iminosugars **1d** and **1e** were found to exist in the half chair (**A2**) and boat or twist boat (**B2**) conformations respectively. This observation was substantiated by employing density functional theory (DFT).

Thus, the different conformers of **1d** and **1e** were generated by varying the C4–C5–C6–N1 and C2–N1–C6–C5 dihedral angles from −80° to +80° within the framework of HF/3-21G(d) theory. The corresponding energy profiles are displayed in Fig. 19S and 20S, of the supporting information. As revealed from these profiles, ring conformers with chair (C), half chair (HC), twisted chair (TC) and twisted boat (TB) were encompassed. Minima (24 for **1d** and 20 for **1e**) on the potential energy surface using the dihedral angle as reaction coordinate, were optimized at the B3LYP/6-31G(d,p) level of theory. Stationary point geometries thus obtained were confirmed to be local minima from the vibrational frequencies, all of which turn out to be real. Relative stabilization energies (ΔE_{Rel}) were calculated by subtracting the energy of lowest energy conformer from those of rest of the conformers (Table 2S in Supporting Information). Some of these geometries from the scan of both the C4–C5–C6–N1 and C2–N1–C6–C5 dihedral angles exhibiting different hydrogen bonding patterns finally converged to identical conformers. Out of several local minima possessing similar six membered ring conformations as well as the orientation of OH group, one conformer was chosen for subsequent calculations. The gas phase structures were reoptimized employing the SCRF-PCM model using water as solvent. The ΔE_{Rel} and Boltzmann contribution (BC) values in the gas phase as well as in water are given in Table 3S in the supporting information specifying the ring conformation. As may be noted **1d** is present in chair (C) and half chair (HC) forms and **1e** exhibits twist boat (TB) and twist chair (TC) ring conformations. Furthermore **1d** conformers with the BC values > 5% in water possess the $^1C_4$ ring conformation, whereas the $^2TB_5$ conformation is noticed in the case of **1e**. The conformers **1d_A112**, **1d_A119**, **1d_A211** and **1d_D111** reveal similar structures except for the orientation of the hydroxyl group. Similar inferences may be drawn for **1e_A206**, **1e_B206**, and **1e_D207** conformers. Lowest energy conformers **1d_A119** and **1e_A206** are shown in Fig. 3 where both views top

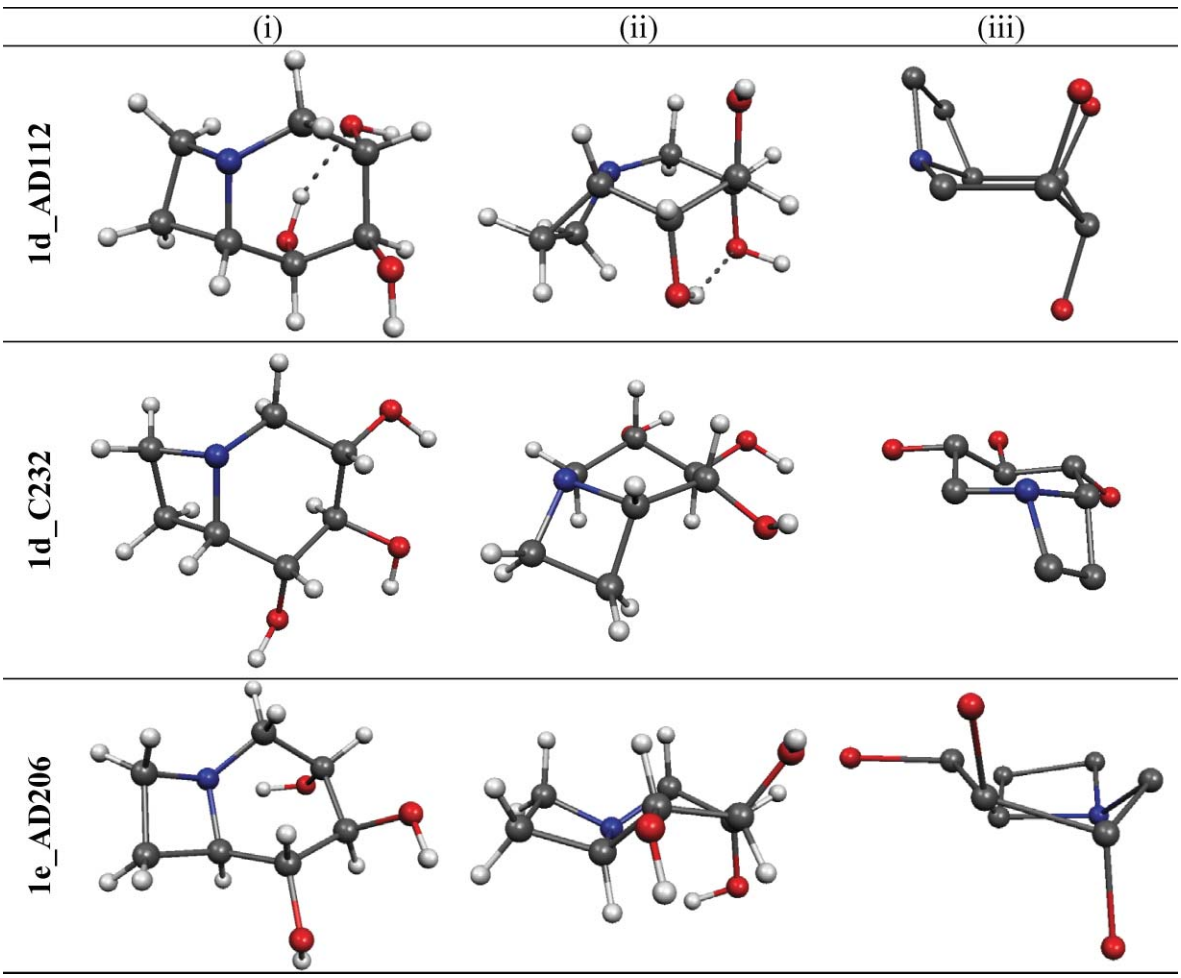

Fig. 3 Optimized geometries of **1d** and **1e** in water. Views from (i) the top, (ii) along the C2–C3 bond are shown (iii) ring conformations ($^1C_4$, ^3HC and $^2TB_5$ respectively) are displayed.

and side along the C2–C3 bond are displayed along with the ring conformations. Thus the $^1C_4$ conformation of **1d** is transparent; **1e** on the other hand exhibits the $^2TB_5$ ring conformation. It should be remarked here that the configuration around the C2–C3 bond is different in **1d** and **1e** diastereomers. The dihedral angle H–C3–C4–H turns out to be 67° here compared to 98° in **1e** with the near eclipsed conformer. Furthermore, the conformer **1d_C232** is predicted to possess the half chair ring conformation (^{3}HC) as inferred from the experiments. The calculated coupling constants for the minimum energy **1d_A112** conformer and that inferred from experiments **1d_C232** and **1e_A206** are given in Table 5S in the supporting information. In case of conformer **1d_C232**, coupling constants for H-2a and H-2e ($J_{2a,3}$ and $J_{2e,3}$) are 9.11 and 4.20 Hz which matches well with 11.0 and 5.0 Hz, respectively, as observed in the experimental NMR spectra of **1d**. While for **1d_A112**, the calculated values of the coupling constants were found to be 1.37 and 3.27 Hz and thus deviate largely from experimental values. In addition, for conformer **1d_C232** the calculated $J_{3,4} = 7.52$ Hz and $J_{4,5} = 7.33$ Hz values for the H-4 were matching well with the experimentally observed value of 6.9 Hz. The large coupling constant values suggested that the H-3 and H-5 protons are *trans* to H-4 (dihedral angle H–C3–C4–H and H–C4–C5–H being ~180°). Thus, the ^{1}H NMR data of **1d_C232** in the ^{3}HC ring conformation matches well with the experimental values corresponding to the half chair conformation of **1d**.

In case of compound **1e**, the experimental coupling constants for H-2 were observed to be $J_{2a,3} = 6.0$ Hz and $J_{2e,3} = 3.3$ Hz. A similar trend has been observed for the calculated coupling constant of **1e_A206** conformer for which the coupling constants for these protons are predicted to be 3.45 Hz and 1.41 Hz, respectively. The lower coupling constant for the $J_{2e,3}$ is in agreement with the experiments. Similar observation may also be made for the coupling constant of H-4. Thus, coupling constant data suggests that the compound **1e** (**1e_A206**) is present in the twisted boat ($^2TB_5$) conformation.

Computational methods

The conformations of **1d** and **1e** possessing different intramolecular hydrogen bonded networks were optimized at the Hartree–Fock (HF/3-21G) level of theory using the Gaussian03 package.[25] The conformers possessing unique hydrogen bonding patterns were labeled with notations A, B, C, and D (*cf.* Fig. 17S in supporting information). Other ring conformations *viz*. chair, twist chair, half chair, twist boat, and boat forms, were generated by scanning the C5–C6–N1–C2 and C4–C5–C6–N1 dihedral angle from –80.0° to 80.0°. Minima on the scanned potential energy surface of both the dihedral angles were identified and further optimized at B3LYP/6-31G(d,p) level of theory by relaxing all the geometrical constraints.[26,27] Relative stabilization energies (ΔE_{Rel}) were calculated by subtracting the energy of lowest energy conformer from those of rest of the conformers. Amongst the conformers having different ΔE_{Rel} only one conformer that possesses the same ΔE_{Rel} values and the same geometry is considered for the calculations hereafter. Self consistent reaction field theory was utilized to investigate the influence of solvent on the conformational energies of **1d** and **1e**.

The gas phase structures were optimized in water employing the polarizable continuum model (PCM)[28] to account for the geometry relaxation in the presence of solvent. The NMR chemical shifts were calculated from the gauge invariant atomic orbital method by subtracting the nuclear magnetic shielding tensors of protons in conformers **1d** and **1e** from that of the protons in TMS.[29] The DFT investigations revealed that the calculated ^{1}H NMR chemical shifts in solvent using the SCRF-PCM model agree better with the experimental ones than those from the gas phase.[30–32] In the case of glucose, it has been pointed out that the accuracy of ^{1}H chemical shifts is affected significantly by the solute geometry and the SCRF models suffice to describe the effect of solvent on the shielding constants.[30] Boltzmann contributions (BC) of these conformers were estimated from the relative stabilization energy values in the gas phase and water. The calculated BC values provide the valuable information regarding relative population of different conformers.

Table 2 IC_{50} values of **1d** and **1e** in mM

Compound	α-Galactosidase	α-Mannosidase	α-Glucosidase	α-Amylase
1d	NI	322.6 ± 0.12	465.8 ± 0.22	110.6 ± 0.03
1e	60 ± 0.03	33.6 ± 0.09*	270.3 ± 0.06	126.5 ± 0.02

NI = No inhibition under assay conditions. The data is indicated as the mean ± SEM; ($n = 3$). (*) denotes a more significant value ($P < 0.05$).

Biological activity

The glycosidase inhibitory activity was studied with different glycosidases.[33] As shown in Table 2, glycosidase inhibition studies of the target compounds revealed that compound **1d** showed no inhibition with α-galactosidase (E.C. 3.2.1.22) and moderate inhibition with both α-mannosidase (E.C. 3.2.1.24) and α-glucosidase (E.C. 3.2.1.20) while **1e** showed selective inhibition against α-mannosidase and moderate inhibition against α-galactosidase and α-glucosidase in the millimolar range. Compounds **1d** and **1e** were also found to have moderate inhibition against α-amylase (E.C. 3.2.1.1) (Table 2). As a reference, porcine pancreatic α-amylase[34] with 0.21 U min^{-1} was taken as 100% enzymatic activity.

Molecular docking

Biological activity was supported by a docking study in order to understand the interactions between compound **1e** and the amino acid residues of mannosidase. Mannosidases are lectin binding proteins and *N*-glycans of α-mannosidase have unique topologies, important functions in protein folding, oligomerization or enzyme activity.[35] The complete sequence of jack bean mannosidase is yet to be reported. Therefore, it is difficult to compare the active sites of the mannosidase from jack bean and ER. Hence, for this study, we have chosen human mannosidase (PDB: 1FO3) as our target structure to perform the molecular docking studies. The template structure of human mannosidase is used to dock the ligand **1e** into the binding pocket of mannosidase. This might provide an insight into the interaction of **1e** with mannosidase from Jack Bean. The active site was predicted by using WHAT IF software. The AUTODOCK 3.0[36] program was used to perform an automatic docking exploration for different conformations of the ligand in the model. The interactions between compound **1e** and human mannosidase (PDB: 1FO3) are given in the Fig. 23S in

Table 3 The total energy (E_{total}), Van der Waals energy (E_{vdw}) and electrostatic energy (E_{ele}) between interacting residues of compound **1e** and human mannosidase (PDB: 1FO3)

Residue	E_{total}/kcal mol^{-1}	E_{vdw}/kcal mol^{-1}	E_{elec}/kcal mol^{-1}
Ser158	−50.101	−1.45	−48.65
Thr446	25.131	−12.27	24.06
Lys229	254.120	−15.71	257.61
Ser222	92.476	−6.65	82.41
Glu225	256.171	−20.30	262.41

the supporting information. Interactions were observed between **1e** and Ser158, Thr446, Lys229, Ser222, Glu225. It shows that **1e** may have significant interaction with mannosidase and may act as an inhibitor. The total binding energies are given in Table 3. The total energy of the complex is 133.50 kcal mol^{-1} with the total electrostatic energy being −27.07 kcal mol^{-1} and total Van der Waals interaction energy −106.44 kcal mol^{-1}.

Conclusion

We have synthesized a new class of iminosugars *viz*. conidine iminosugars **1d** and **1e** with an overall yield of 41% and 37%, respectively, from D-glucose. Reduction of sugar derived β-lactam to azetidine was achieved which is less common in sugar moiety due to acid labile 1,2-acetonide protection. Hydrogenolysis was achieved without destruction of the constrained azetidine ring which is otherwise already reported in the literature. The experimental and DFT calculated ^{1}H coupling constant data suggests that compound **1d** should be assigned the half chair conformation whereas compound **1e** has the twist boat conformation. Compound **1e** was found to have inhibitory activity against α-mannosidase at the mM range whereas compound **1d** was found to be a moderate inhibitor of α-mannosidase and α-glucosidase at the same concentration. Molecular docking studies could successfully correlate interaction energies calculated from the docked poses of the ligands with experimental binding affinities which offer a possible structural rationale for the inhibition mechanism of the conidine iminosugars, **1d** and **1e**. It is noteworthy that **1d** and **1e** inspite of being diastereomers of the same conidine iminosugar showed differential inhibition against α-mannosidase that supports that stereochemistry of the ring fusion proton in conidine iminosugars is significant in glycosidase inhibition.

Experimental section

General experimental methods

Melting points were recorded with a Thomas Hoover melting point apparatus and are uncorrected. IR spectra were recorded with a Shimadzu FTIR-8400 as a thin film or in nujol mull or using KBr pellets and are expressed in cm^{-1}. ^{1}H (300 MHz) and ^{13}C (75 MHz) NMR spectra were recorded on a Varian Mercury 300 using $CDCl_3$/D_2O as solvent. Chemical shifts were reported in δ unit (ppm) with reference to TMS as an internal standard and J values are given in Hz. Assignments of the signals were confirmed by decoupling experiments. Elemental analyses were carried out with an Elemental Analyser Flash 1112. Optical rotations were measured using a JASCO P-1020 polarimeter with sodium light (589.3 nm). Thin layer chromatography was performed on pre-coated plates (0.25 mm, silica gel 60 F254). Column chromatography was carried out with silica gel (100–200 mesh). The reactions were carried out in oven-dried glassware under dry N_2. Methanol, THF, dichloromethane were purified and dried before use. After decomposition of the reaction mixture, the work-up involves extraction with solvent, washing of combined organic layer with water, brine, drying over anhydrous sodium sulfate and evaporation of solvent under reduced pressure below 50 °C.

1,2-*O*-Isopropylidene-3-*O*-benzyl-5,6-dideoxy-5-(*N*-benzylamino)-β-L-*ido*-heptofuranuronic acid (3a)

To an ice cooled solution of β-L-*ido*-β-amino ester **2a** (0.200 g, 0.44 mmol) in methanol–water (5 cm^3, 4/1) was added lithium hydroxide monohydrate (0.112 g, 2.66 mmol) at 0 °C. The mixture was brought to 25 °C, stirred for 2.5 h and neutralized to pH 7 by addition of 0.5 M H_3PO_4. Methanol was evaporated and residue was extracted with chloroform (3 × 7 cm^3), the combined chloroform layer was washed with water, dried with anhydrous Na_2SO_4 and the solvent removed under reduced pressure to give a pale yellow solid which on purification by column chromatography (chloroform–methanol = 9.5/0.5) afforded β-L-*ido*-heptofuranuronic acid **3a** (0.184 g, 98%) as a white solid (Found: C, 67.09; H, 6.94; N, 3.23. Calc for $C_{24}H_{29}NO_6$: C, 67.43; H, 6.84; N, 3.28%); R_f 0.30 (chloroform–methanol = 9/1); $[\alpha]_D^{32}$ −32.17 (*c* 1.08, in $CHCl_3$); mp 165–166 °C; ν_{max} (neat)/cm^{-1} 3445 (CO*OH*), 1611 (*NH*), 2928, 1084; δ_H (300 MHz; $CDCl_3$; Me_4Si) 1.32 (3H, s, C*H*$_3$), 1.48 (3H, s, C*H*$_3$), 2.20 (1H, dd, *J* 17.1 and 5.1 Hz, *H*-6a), 2.58 (1H, dd, *J* 17.1 and 4.95 Hz, *H*-6b), 3.30–3.56 (1H, m, *H*-5), 3.88 (1H, d, *J* 12.7 Hz, NC*H*$_2$Ph), 3.98 (1H, d, *J* 3.0 Hz, *H*-3), 4.02 (1H, d, *J* 12.7 Hz, NC*H*$_2$Ph), 4.25 (1H, dd, *J* 9.5 and 3.0 Hz, *H*-4), 4.48 (1H, d, *J* 11.7 Hz, OC*H*$_2$Ph), 4.67 (1H, d, *J* 3.6 Hz, *H*-2), 4.69 (1H, d, *J* 11.7 Hz, OC*H*$_2$Ph), 5.94 (1H, d, *J* 3.6 Hz, *H*-1), 7.23–7.45 (10H, m, Ar-*H*) 7.40–8.20 (2H, br, Exchangeable with D_2O, N*H* and COO*H*); δ_C (75 MHz; $CDCl_3$; Me_4Si) 26.1 (*C*H$_3$), 26.7 (*C*H$_3$), 31.3 (*C*-6), 50.2 (*C*-5), 53.3 (N*C*H$_2$Ph), 72.0 (O*C*H$_2$Ph), 80.3, 81.1, 81.7 (*C*-2/*C*-3/*C*-4), 101.8 (*C*-1), 112.2 (O*C*O), 128.2, 128.4, 128.7, 128.9, 135.9, 136.5 (Ar-*C*), 172.6 (*C*OOH).

1,2-*O*-Isopropylidene-3-*O*-benzyl-5,6-dideoxy-5-(*N*-benzylamino)-α-D-*gluco*-heptofuranuronic acid (3b)

Following the same procedure, α-D-*gluco*-β-amino ester **2b** (0.250 g, 0.55 mmol) was hydrolyzed with LiOH·H_2O (0.140 g, 3.34 mmol) in methanol–water (5 cm^3, 4/1) for 3 h to give the α-D-*gluco*-heptofuranuronic acid **3b** (0.225 g, 96%) after silica gel column purification (chloroform–methanol = 9.5/0.5) as a white solid (Found: C, 66.94; H, 6.78; N, 3.11. Calc for $C_{24}H_{29}NO_6$: C, 67.43; H, 6.84; N, 3.28%); R_f 0.30 (chloroform–methanol = 9/1); $[\alpha]_D^{32}$ −5.75 (*c* 1.02, in $CHCl_3$); mp 162–163 °C; ν_{max}(neat)/cm^{-1} 3438 (CO*OH*), 1625 (*NH*), 2938, 1062; δ_H (300 MHz; $CDCl_3$; Me_4Si) 1.34 (3H, s, C*H*$_3$), 1.49 (3H, s, C*H*$_3$), 2.17 (1H, dd, *J* 15.3 and 11.0 Hz, *H*-6a), 2.48 (1H, dd, *J* 15.3 and 4.0 Hz, *H*-6b), 3.55 (1H, dt, *J* 11.0 and 4.0 Hz, *H*-5), 3.82 (1H, d, *J* 12.3 Hz, NC*H*$_2$Ph), 4.09 (1H, d, *J* 3.3 Hz, *H*-3), 4.16 (1H, d, *J* 12.3 Hz, NC*H*$_2$Ph), 4.18 (1H, dd, *J* 4.7 and 3.3 Hz, *H*-4), 4.46 (1H, d, *J* 11.4 Hz, OC*H*$_2$Ph), 4.64 (1H, d, *J* 3.9 Hz, *H*-2), 4.68 (1H, d, *J* 11.4 Hz, OC*H*$_2$Ph), 6.05 (1H, d, *J* 3.9 Hz, *H*-1), 6.20–6.90 (2H, br, Exchangeable with

D_2O, N*H* and COO*H*), 7.15–7.38 (10H, m, Ar-*H*); δ_C (75 MHz; $CDCl_3$; Me_4Si) 26.1 (*C*H_3), 26.7 (*C*H_3), 33.2 (*C*-6), 51.4 (*C*-5), 53.6 (N*C*H_2Ph), 71.9 (O*C*H_2Ph), 79.3, 81.2, 82.1 (*C*-2/*C*-3/*C*-4), 104.5 (*C*-1), 112.1 (O*C*O), 128.2, 128.3, 128.5, 128.8, 128.9, 135.9, 135.9 (Ar-*C*), 173.2 (*C*OOH).

1,2-*O*-Isopropylidene-3-*O*-benzyl-5,6-dideoxy-5,7-(*N*-benzylimino)-β-L-*ido*-sept-1,4-furan-7-ulose (4a)

To a suspension of 2-chloro-1-methylpyridinium iodide (0.329 g, 1.29 mmol) and Et_3N (0.359 cm^3, 2.58 mmol) in dry dichloromethane (6 cm^3) at 25 °C was added a solution of β-L-*ido*-heptofuranuronic acid **3a** (0.500 g, 1.17 mmol) in dry dichloromethane (2 cm^3) drop wise. The solution was stirred at 25 °C for 2 h and water (2 cm^3) was added. The reaction mixture was extracted with ethyl acetate (3 × 10 cm^3), the organic layer dried on anhydrous Na_2SO_4 and the solvent removed under reduced pressure to give a thick liquid which on column purification (n-hexane–ethyl acetate = 8.5/1.5) afforded β-L-*ido*-β-lactam **4a** (0.430 g, 89%) as white crystalline solid (Found: C, 70.58; H, 6.55; N, 3.38. Calc for $C_{24}H_{27}NO_5$: C, 70.40; H, 6.65; N, 3.42%); R_f 0.45 (n-hexane–ethyl acetate = 7/3); $[\alpha]_D^{32}$ −39.86 (*c* 2.61, in $CHCl_3$); mp 129–131 °C; ν_{max} (neat)/cm^{-1} 1748 (*C*=*O*), 1065, 1380; δ_H (300 MHz; $CDCl_3$; Me_4Si) 1.27 (3H, s, C*H*$_3$), 1.42 (3H, s, C*H*$_3$), 2.37 (1H, dd, *J* 14.6 and 2.5 Hz, *H*-6a), 2.83 (1H, dd, *J* 14.6 and 5.2 Hz, *H*-6b), 3.79 (1H, ddd, *J* 8.5, 5.2 and 2.5 Hz, *H*-5), 3.87 (1H, d, *J* 3.6 Hz, *H*-3), 4.11 (1H, dd, *J* 8.5 and 3.6 Hz, *H*-4), 4.22 (1H, d, *J* 14.7 Hz, NC*H*$_2$Ph). 4.35 (1H, d, *J* 12.3 Hz, OC*H*$_2$Ph), 4.58 (1H, d, *J* 3.6 Hz, *H*-2), 4.64 (1H, d, *J* 14.7 Hz, NC*H*$_2$Ph), 4.67 (1H, d, *J* 12.3 Hz, OC*H*$_2$Ph), 5.98 (1H, d, *J* 3.6 Hz, *H*-1), 7.18–7.40 (10H, m, Ar-*H*); δ_C (75 MHz; $CDCl_3$; Me_4Si) 26.2 (*C*H_3), 26.7 (*C*H_3), 39.0 (*C*-6), 45.6 (N*C*H_2Ph), 49.7 (*C*-5), 71.7 (O*C*H_2Ph), 81.6, 81.8,83.7 (*C*-2/*C*-3/*C*-4), 105.7 (*C*-1), 111.8 (O*C*O), 127.3, 128.1, 128.3, 128.5, 128.5, 128.6, 136.5, 136.6 (Ar-*C*), 165.9 (*C*O).

1,2-*O*-Isopropylidene-3-*O*-benzyl-5,6-dideoxy-5,7-(*N*-benzylimino)-α-D-*gluco*-sept-1,4-furan-7-ulose (4b)

As above, the reaction of α-D-*gluco*-heptofuranuronic acid **3b** (0.700 g, 1.64 mmol) with 2-chloro-1-methylpyridinium iodide (0.461 g, 1.80 mmol) and Et_3N (0.503 cm^3, 3.61 mmol) in dry dichloromethane (10 cm^3) at 25 °C for 3 h gave a thick liquid which on silica gel column purification (n-hexane–ethyl acetate = 8.7/1.3) afforded α-D-*gluco*-β-lactam **4b** (0.610 g, 91%) as a white solid (Found: C, 70.68; H, 6.43; N, 3.35. Calc for $C_{24}H_{27}NO_5$: C, 70.40; H, 6.65; N, 3.42%); R_f 0.45 (n-hexane–ethyl acetate = 7/3); $[\alpha]_D^{32}$ −38.38 (*c* 2.58, in $CHCl_3$); mp 126–127 °C; ν_{max} (neat)/cm^{-1} 1744 (*C*=*O*), 1080, 1385; δ_H (300 MHz; $CDCl_3$; Me_4Si) 1.23 (3H, s, C*H*$_3$), 1.40 (3H, s, C*H*$_3$), 3.03 (1H, dd, *J* 14.7 and 4.9 Hz, *H*-6a), 3.15 (1H, dd, *J* 14.7 and 2.4 Hz, *H*-6b), 3.66 (1H, d, *J* 3.6 Hz, *H*-3), 3.83 (1H, dt, *J* 4.9 and 2.4 Hz, *H*-5), 4.18 (1H, dd, *J* 4.9 and 3.6 Hz, *H*-4), 4.28 (1H, d, *J* 15.6 Hz, NC*H*$_2$Ph), 4.30 (1H, d, *J* 12.0 Hz, OC*H*$_2$Ph), 4.45 (1H, d, *J* 15.6 Hz, NC*H*$_2$Ph), 4.57 (1H, d, *J* 3.9 Hz, *H*-2), 4.59 (1H, d, *J* 12.0 Hz, OC*H*$_2$Ph), 5.89 (1H, d, *J* 3.9 Hz, *H*-1), 7.18–7.40 (10H, m, Ar-*H*); δ_C (75 MHz; $CDCl_3$; Me_4Si) 26.2 (*C*H_3), 26.7 (*C*H_3), 40.2 (*C*-6), 44.8 (N*C*H_2Ph), 50.0 (*C*-5), 71.4 (O*C*H_2Ph), 78.6, 81.8, 82.3 (*C*-2/*C*-3/*C*-4), 104.7 (*C*-1), 111.7 (O*C*O), 127.2, 127.5, 127.6, 127.9, 128.4, 128.6, 136.1, 137.0 (Ar-*C*), 168.0 (*C*O).

1,2-*O*-Isopropylidene-3-*O*-benzyl-5,6,7-trideoxy-5,7-(*N*-benzylimino)-β-L-*ido*-sept-1,4-furanose (5a)

To a cooled suspension (ice–salt mixture) of $LiAlH_4$ (0.014 g, 0.36 mmol) in anhydrous THF (2 cm^3) was added a solution of $AlCl_3$ (0,016 g, 0.12 mmol) in anhydrous THF (2 cm^3) and stirred at −10 °C for 30 min. Then a solution of β-L-*ido*-β-lactam **4a** (0.100 g, 0.24 mmol) in anhydrous THF (3 cm^3) was added drop wise at −10 °C for 5 min and further stirred for 10 min at 0 °C. The reaction was quenched with saturated aqueous Na_2SO_4 at 0 °C slowly. The reaction mixture was filtered through celite, solvent removed under reduced pressure to give a colorless oil which was chromatographed (n-hexane–ethyl acetate = 8.8/1.2) to give β-L-*ido*-azetidine **5a** (0.082 g, 83%) as a white solid (Found: C, 72.97; H, 7.46; N, 3.60. Calc for $C_{24}H_{29}NO_4$: C, 72.89; H, 7.39; N, 3.54%); R_f 0.50 (n-hexane–ethyl acetate = 7/3); $[\alpha]_D^{32}$ −131.68 (*c* 2.14, in $CHCl_3$); mp 94–96 °C; ν_{max} (neat)/cm^{-1} 1060, 1375; δ_H (300 MHz; $CDCl_3$; Me_4Si) 1.33 (3H, s, C*H*$_3$), 1.53 (3H, s, C*H*$_3$), 1.82–1.94 (2H, m, *H*-6a and *H*-6b), 2.76–2.88 (1H, m, *H*-7a), 3.13–3.24 (1H, m, *H*-7b), 3.37 (1H, d, *J* 12.6 Hz, NC*H*$_2$Ph), 3.60 (1H, m, *H*-5), 3.89 (1H, d, *J* 3.3 Hz, *H*-3), 4.09 (1H, d, *J* 12.6 Hz, NC*H*$_2$Ph), 4.38 (1H, dd, *J* 4.9 and 3.3 Hz, *H*-4), 4.42 (1H, d, *J* 12.0 Hz, OC*H*$_2$Ph), 4.59 (1H, d, *J* 3.7 Hz, *H*-2), 4.66 (1H, d, *J* 12.0 Hz, OC*H*$_2$Ph), 5.99 (1H, d, *J* 3.7 Hz, *H*-1), 7.18–7.40 (10H, m, Ar-*H*); δ_C (75 MHz; $CDCl_3$; Me_4Si) 20.0 (*C*-6), 26.4 (*C*H_3), 26.8 (*C*H_3), 51.2 (*C*-7), 62.4 (*C*-5), 64.3 (N*C*H_2Ph), 71.8 (O*C*H_2Ph), 81.6, 81.8, 84.8 (*C*-2/*C*-3/*C*-4), 105.4 (*C*-1), 111.5 (O*C*O), 126.8, 127.7, 127.8, 128.1, 128.3, 128.5, 128.9, 137.1, 137.6 (Ar-*C*).

1,2-*O*-Isopropylidene-3-*O*-benzyl-5,6,7-trideoxy-5,7-(*N*-benzylimino)-α-D-*gluco*-sept-1,4-furanose (5b)

The reduction of α-D-*gluco*-β-lactam **4b** (0.500 g, 1.22 mmol) with $LiAlH_4$ (0.070 g, 1.83 mmol) and $AlCl_3$ (0.082 g, 0.61 mmol) in anhydrous THF (10 cm^3) at −10 °C to 0 °C in 15 min gave the colorless oil which on column purification (n-hexane–ethyl acetate = 9/1) afforded α-D-*gluco*-azetidine **5b** (0.410 g, 85%) as a white solid (Found: C, 72.74; H, 7.28; N, 3.43. Calc for $C_{24}H_{29}NO_4$: C, 72.89; H, 7.39; N, 3.54%); R_f 0.50 (n-hexane–ethyl acetate = 7/3); $[\alpha]_D^{32}$ −24.43 (*c* 2.12, in $CHCl_3$); mp 101–103 °C; ν_{max} (neat)/cm^{-1} 1070, 1355; δ_H (300 MHz; $CDCl_3$; Me_4Si) 1.31 (3H, s, C*H*$_3$), 1.44 (3H, s, C*H*$_3$), 2.08–2.16 (1H, m, *H*-6a), 2.24–2.41 (1H, m, *H*-6a), 2.84-2.88 (1H, m, *H*-7a), 3.35 (1H, td, *J* 9.0, 2.4 Hz, *H*-7b), 3.50 (1H, d, *J* 12.9 Hz, NC*H*$_2$Ph), 3.56–3.70 (2H, m, NC*H*$_2$Ph, *H*-5), 3.81 (1H, d, *J* 3.0 Hz, *H*-3), 4.06 (1H, dd, *J* 6.0 and 3.0 Hz, *H*-4), 4.38 (1H, d, *J* 12.0 Hz, OC*H*$_2$Ph), 4.60 (1H, d, *J* 3.9 Hz, *H*-2), 4.62 (1H, d, *J* 12.0 Hz, OC*H*$_2$Ph), 5.91 (1H, d, *J* 3.9 Hz, *H*-1), 7.18-7.40 (10H, m, Ar-*H*), δ_C (75 MHz; $CDCl_3$; Me_4Si) 21.1 (*C*-6), 26.4 (*C*H_3), 26.7 (*C*H_3), 52.4 (*C*-7), 62.7 (*C*-5), 63.4 (N*C*H_2Ph), 71.2 (O*C*H_2Ph), 81.8, 82.0, 82.6 (*C*-2/*C*-3/*C*-4), 104.8 (*C*-1), 111.5 (O*C*O), 126.9, 127.4, 127.8, 128.0, 128.2, 128.4, 128.7, 137.4, 138.4 (Ar-*C*).

(3*S*,4*R*,5*R*,6*S*)-3,4,5-Trihydroxy-conidine (1d)

A cooled (0 °C) solution of **5a** (0.41 g, 1.04 mmol) in TFA–H_2O (5 cm^3, 3 : 2) was stirred for 1 h, brought to 25 °C, and stirred for additional 2 h. TFA was evaporated at high vacuum to yield the crude hemiacetal (0.32 g). A solution of the above product in dry methanol (8 cm^3) was hydrogenated in the presence of

10% Pd/C (0.07 g) at 80 psi for 5 days. The catalyst was filtered and washed with methanol, and the filtrate was concentrated to afford a thick liquid. Purification by column chromatography on silica gel chloroform–methanol (5.5/4.5) afforded **1d** (0.13 g, 78%) as a moisture sensitive colorless solid (Found: C, 52.76; H, 8.16; N, 8.87. Calc for $C_7H_{13}NO_3$: C, 52.82; H, 8.23; N, 8.80%); R_f 0.30 (methanol); $[\alpha]_D^{32}$ −36.43 (*c* 1.12, MeOH); ν_{max} (neat)/cm^{-1} 3600–3200 (broad, OH); δ_H (300 MHz; D_2O; Me_4Si) 2.44–2.58 (1H, m, *H*-7a), 2.78–2.96 (1H, m, *H*-7b), 3.34 (1H, dd, *J* 12.6 and 11.0 Hz, *H*-2a), 3.63 (1H, dd, *J* 12.6 and 5.0 Hz, *H*-2b), 3.67–3.76 (1H, m, *H*-6), 3.82 (1H, dt, *J* 10.0 and 4.7 Hz, *H*-8a), 3.90 (1H, t, *J* 6.9 Hz, *H*-4), 3.95 (1H, dd, *J* 6.9 Hz, *H*-5), 4.45 (1H, dt, *J* 10.0 and 8.8 Hz, *H*-8b), 4.88–5.05 (1H, m, merged with HDO signal, *H*-3); δ_C (75 MHz; D_2O; Me_4Si) 22.2 (*C*-7), 49.3 (*C*-8), 53.7 (*C*-6), 62.9 (*C*-2), 68.3 (*C*-3), 71.5 (*C*-5), 73.7 (*C*-4).

(3*S*,4*R*,5*R*,6*R*)-3,4,5-Trihydroxy-conidine (1e)

Following a similar procedure, compound **5b** (0.35 g, 0.89 mmol) was treated with TFA–H_2O (5 cm^3, 3 : 2), and the resultant hemiacetal was hydrogenated over 10% Pd/C (0.05 g) for 5 days to furnish, after isolation and purification by column chromatography on silica gel (chloroform–methanol = 7.5/2.5), compound **1e** (0.1 g, 71%) as a moisture sensitive colorless solid (Found: C, 52.89; H, 8.33; N, 8.77. Calc for $C_7H_{13}NO_3$: C, 52.82; H, 8.23; N, 8.80%); R_f 0.45 (chloroform–methanol = 5/5); $[\alpha]_D^{32}$ +44.21 (*c* 1.12, MeOH); ν_{max} (neat)/cm^{-1} 3600–3200 (broad, OH); δ_H (300 MHz; D_2O; Me_4Si) 2.34–2.50 (1H, m, *H*-7a), 2.74–2.90 (1H, m, *H*-7b), 3.25 (1H, dd, *J* 13.5 and 6.0 Hz, *H*-2a), 3.43 (1H, dd, *J* 13.5 and 3.3 Hz, *H*-2b), 3.56 (1H, dd, *J* 8.2 and 4.8 Hz, *H*-4), 4.06–4.14 (1H, m, *H*-3), 4.14–4.27 (3H, m, *H*-5, *H*-8a, *H*-8b), 4.27–4.36 (1H, m, *H*-6); δ_C (75 MHz; D_2O; Me_4Si) 18.8 (*C*-7), 50.2 (*C*-8), 55.0 (*C*-6), 61.3 (*C*-2), 67.2 (*C*-3), 68.3 (*C*-5), 73.4 (*C*-4).

General procedure for glycosidase inhibition assay

Glycosidase inhibition assay of conidine iminosugars **1d** and **1e** was carried out by mixing 0.1 U cm^{-3} each of α-galactosidase, α-mannosidase and α-glucosidase with the samples and incubated for 1 h at 37 °C. Enzyme action for α-galactosidase was initiated by addition of 10 mM *p*-nitrophenyl-α-D-galactopyranoside (*p*NPG) as a substrate in 200 mM sodium acetate buffer. The reaction was incubated at 37 °C for 10 min and stopped by adding 2 cm^3 of 200 mM borate buffer of pH 9.8. α-Mannosidase activity was initiated by addition of 10 mM *p*-nitrophenyl-α-D-mannopyranoside as a substrate in 100 mM citrate buffer of pH 4.5. The reaction was incubated at 37 °C for 10 min and stopped by adding 2 cm^3 of 200 mM borate buffer of pH 9.8. Initiation of α-glucosidase activity was done by addition of 10 mM *p*-nitrophenyl-α-D-glucopyranoside in 100 mM phosphate buffer of pH 6.8 and stopped by adding 2 cm^3 of 0.1 M Na_2CO_3 after an incubation of 10 min at 37 °C. α-Glycosidase activity was determined by measuring absorbance of the *p*-nitrophenol released from *p*NPG at 420 nm using Shimadzu Spectrophotometer UV-1601. One unit of glycosidase activity is defined as the amount of enzyme that hydrolyzed 1 μM of *p*-nitrophenyl pyranoside per minute under assay condition.

General procedure for α-amylase inhibition assay

Amylase activity was assayed using a modified Bernfeld method (1955) using starch as substrate. 50 μg cm^{-3} (O. D. adjusted to 0.4 at 280 nm) of porcine pancreatic α-amylase was incubated with 5 mg cm^{-3} samples at 37 °C for 10 min. One percent starch was used as substrate. The samples without α-amylase were used as controls and the test reading was subtracted from the absorbance of these controls. The reducing sugar was estimated using DNSA assay at 540 nm and the enzyme units were expressed as micro-molar per minute. One unit of enzyme was defined as the amount of enzyme required to liberate 1 μM of maltose under assay conditions. The final inhibition shown by different samples were compared with the standard inhibitor, acarbose.

Statistical analysis

The statistical analysis was performed using one way analysis of variance (ANOVA) and two tailed *t*-test ($P < 0.05$). Results are expressed as means ± SEM.

Molecular docking

Interactions of compound **1e** against amino acid residues of human mannosidase (PDB: 1FO3) were found out by employing molecular docking studies. The active site was predicted by using WHAT IF software. The AUTODOCK 3.0 program was used to perform an automatic docking exploration for different conformations of the ligand in the model. AUTODOCK 3.0 uses three search methods [a genetic algorithm, a local search method, and an adaptive global–local search method based on Lamarckian genetics (LGA)] in conjunction with an empirical force field that allows the prediction of binding free energies for docked ligand. The optimized autodocking run parameters are as follows: the maximum number of energy evaluations was increased to 2 500 000 per run; the maximum number of generation in the genetic algorithm was increased to 100 000; and the number of GA run was 100. The binding pocket consists mainly of glutamate residues that make the site very active. Distances between polar atoms less than 3.6 Å may be regarded as hydrogen bonds and interactions less than 4.5 Å may be taken as Van der Waals interactions.

Acknowledgements

We are grateful to Prof. M. S. Wadia for helpful discussions. SPS and RVP are thankful to CSIR, New Delhi, for the Junior Research Fellowship and Senior Research Fellowship, respectively. SG is thankful to University of Pune for Research Stipend. AMJ is thankful to UGC for Senior Research Fellowship. We are also thankful to the University of Pune, (BCUD Research Project, 2009-2011) Pune for the financial support.

References

1 B. Winchester, *Glycobiology*, 2005, **15**, 1R–15R.
2 P. E. Goss, M. A. Baker, J. P. Carver and J. W. Dennis, *Clin. Cancer Res.*, 1995, **1**, 935–944.

3 P. E. Goss, C. L. Reid, D. Bailey and J. W. Dennis, *Clin. Cancer Res.*, 1997, **3**, 1077–1086.
4 O. Kazuaki and D. M. Jamey, *Cell*, 2006, **126**, 855–867.
5 T. D. Butters, R. A. Dwek and F. M. Platt, *Chem. Rev.*, 2000, **100**, 4683–4696.
6 H. Gin and V. Rigalleau, *Diab. Metabol.*, 2000, **26**, 265–272.
7 (*a*) E. Truscheit, W. Frommer, B. Junge, L. Muller, D. D. Schmidt and W. Wingender, *Angew. Chem., Int. Ed. Engl.*, 1981, **20**, 744–761; (*b*) R. H. Furneaux, G. J. Gainsford, J. M. Mason, P. C. Tyler, O. Hartley and B. G. Winchester, *Tetrahedron*, 1997, **53**, 245–268.
8 M. J. Humphries, K. Matsumoto, S. L. White and K. Olden, *Cancer Res.*, 1986, **46**, 5215–5222.
9 (*a*) A. Karpas, G. W. J. Fleet, R. A. Dwek, S. Petursson, S. K. Namgoong, N. G. Ramsden, G. S. Jacob and T. W. Rademacher, *Proc. Natl. Acad. Sci. U. S. A.*, 1988, **85**, 9229–9233; (*b*) B. D. Walker, M. Kowalski, W. C. Goh, K. Kozarsky, M. Krieger, C. Rosen, L. Rohrschneider, W. A. Haseltine and J. Sodroski, *Proc. Natl. Acad. Sci. U. S. A.*, 1987, **84**, 8120–8124; (*c*) P. S. Sunkara, D. L. Taylor, M. S. Kang, T. L. Bowlin, P. S. Liu, A. S. Tyms and A. Sjoerdsma, *Lancet*, 1989, **333**, 1206.
10 E. A. McGregor, S. Janecek and B. Svensson, *Biochim. Biophys. Acta*, 2001, **1546**, 1–20.
11 (*a*) H. Nojima, I. Kimura, F.-J. Chen, Y. Sugihara, M. Haruno, A. Kato and N. Asano, *J. Nat. Prod.*, 1998, **61**, 397–400; (*b*) J. A. Balfour and D. McTavish, *Drugs*, 1993, **46**, 1025–1054.
12 P. Compain and O. R. Martin, ed. *Imunosugars: From synthesis to therapeutic applications* Wiley, New York, 2007, ISBN 978-0-470-03391-3.
13 G. Pandey, S. G. Dumbre, M. I. Khan, M. Shabab and V. G. Puranik, *Tetrahedron Lett.*, 2006, **47**, 7923–7926.
14 K. Löffler and P. Plöcker, *Ber.*, 1907, **40**, 1310–1324.
15 V. A. Golenchenko, S. A. Silaeva, A. V. Gavril'chak, A. B. Shekhter, A. Ya. Nikolaev, V. G. Chumakov and V. S. Efimov, *Bull. Exp. Biol. Med.*, 1995, **120**, 1039–1041.
16 (*a*) K. Loffler, *Ber.*, 1909, **42**, 948–960; (*b*) K. Loffler and A. Grosse, *Ber.*, 1907, **40**, 1325–1336.
17 (*a*) D. D. Dhavale, S. D. Markad, N. S. Karanjule and J. Prakashareddy, *J. Org. Chem.*, 2004, **69**, 4760–4766; (*b*) N. S. Karanjule, S. D. Markad, V. S. Shinde and D. D. Dhavale, *J. Org. Chem.*, 2006, **71**, 4667–4670; (*c*) N. S. Karanjule, S. D. Markad and D. D. Dhavale, *J. Org. Chem.*, 2006, **71**, 6273–6276; (*d*) O. P. Bande, V. H. Jadhav, V. G. Puranik and D. D. Dhavale, *Tetrahedron: Asymmetry*, 2007, **18**, 1176–1182; (*e*) V. P. Vyavahare, S. Chattopadhyay, V. G. Puranik and D. D. Dhavale, *Synlett*, 2007, **10**, 559–562; (*f*) O. P. Bande, V. H. Jadhav, V. G. Puranik, D. D. Dhavale and M. Lombardo, *Tetrahedron Lett.*, 2009, **50**, 6906–6908; (*g*) O. P. Bande, V. H. Jadhav, V. G. Puranik and D. D. Dhavale, *Synlett*, 2009, **12**, 1959–1963 and references cited therein.
18 N. T. Patil, J. N. Tilekar and D. D. Dhavale, *J. Org. Chem.*, 2001, **66**, 1065–1074.
19 R. C. Mishra, R. Tripathi, D. Katiyar, N. Tewari, D. Singh and R. P. Tripathi, *Bioorg. Med. Chem.*, 2003, **11**, 5363–5374.
20 H. Huang, N. Iwasawa and T. Mukaiyama, *Chem. Lett.*, 1984, 1465–1466.
21 M. J. Jorgenson, *Tetrahedron Lett.*, 1962, **3**, 559–562.
22 Though there is a report (I. Ojima, M. Zhao, T. Yamato, K. Nakahashi, M. Yamashita and R. Abe *J. Org. Chem.*, 1991, **56**, 5263–5277) that hydrogenolysis of azetidines under similar conditions gives ring opened product, we have not observed any azetidine ring opening product.
23 N. T. Patil, J. N. Tilekar and D. D. Dhavale, *Tetrahedron Lett.*, 2001, **42**, 747–749.
24 G. Pandey, S. G. Dumbre, S. Pal, M. I. Khan and M. Shabab, *Tetrahedron*, 2007, **63**, 4756–4761.
25 M. J. Frisch, G. W. Trucks, H. B. Schlegel, G. E. Scuseria, M. A. Robb, J. R. Cheeseman, J. A. Montgomery Jr., T. Vreven, K. N. Kudin, J. C. Burant, J. M. Millam, S. S. Iyengar, J. Tomasi, V. Barone, B. Mennucci, M. Cossi, G. Scalmani, N. Rega, G. A. Petersson, H. Nakatsuji, M. Hada, M. Ehara, K. Toyota, R. Fukuda, J. Hasegawa, M. Ishida, T. Nakajima, Y. Honda, O. Kitao, Nakai, H. M. Klene, X. Li, J. E. Knox, H. P. Hratchian, J. B. Cross, V. Bakken, C. Adamo, J. J. Aramillo, R. Gomperts, R. E. Stratmann, O. Yazyev, A. J. Austin, R. Cammi, C. Pomelli, J. W. Ochterski, P. Y. Ayala, K. Morokuma, G. A. Voth, P. Salvador, J. J. Dannenberg, V. G. Zakrzewski, S. Dapprich, A. D. Daniels, M. C. Strain, O. Farkas, D. K. Malick, A. D. Rabuck, K. Raghavachari, J. B. Foresman, J. V. Ortiz, Q. Cui, A. G. Baboul, S. J. Clifford, B. B. Cioslowski, G. Stefanov, A. Liu, P. Liashenko, I. Piskorz, R. L. Komaromi, D. J. Martin, T. M. A. Fox, C. Y. Keith, A. Al-Laham, M. Peng, M. Nanayakkara, P. M. W. Challacombe, B. Gill, W. Johnson, M. W. Chen, C. Wong, J. Gonzalez and A. Pople, *Gaussian 03, Revision C.02*, Gaussian, Wallingford, 2004.
26 A. D. Becke, *J. Chem. Phys.*, 1993, **98**, 5648–5652.
27 C. Lee, W. Yang and R. G. Parr, *Phys. Rev. B*, 1988, **37**, 785–789.
28 S. Miertuš, E. Scrocco and J. Tomasi, *Chem. Phys.*, 1981, **55**, 117–129.
29 K. Wolinski, J. F. Hilton and P. Pulay, *J. Am. Chem. Soc.*, 1990, **112**, 8251–8260.
30 A. Bagno, F. Rastrelli and G. Saielli, *J. Org. Chem.*, 2007, **72**, 7373–7381.
31 R. V. Pinjari and S. P. Gejji, *J. Phys. Chem. A*, 2008, **112**, 12679–12686.
32 R. V. Pinjari and S. P. Gejji, *J. Phys. Chem. A*, 2009, **113**, 1368–1376.
33 M. R. Bhandari, A. N. Jong, G. Hong and J. Kawabata, *Food Chem.*, 2008, **106**, 247–252.
34 G. L. Miller, *Anal. Chem.*, 1959, **31**, 426–428.
35 Y. Kimura, D. Hess and A. Sturm, *Eur. J. Biochem.*, 1999, **264**, 168–175.
36 G. M. Morris, D. S Goodsell, R. S. Halliday, R. Huey, W. E. Hart, R. K. Belew and A. J. Olson, *J. Comput. Chem.*, 1998, **19**, 1639–1662.